Inorganic Chemistry

Article

pubs.acs.org/IC

Structure-Directing Effect of Alkali Metal Cations in New Molybdenum Selenites, $Na_2Mo_2O_5(SeO_3)_2$, $K_2Mo_2O_5(SeO_3)_2$, and $Rb_2Mo_3O_7(SeO_3)_3$

Seong-eun Bang and Kang Min Ok*

Department of Chemistry, Chung-Ang University, 84 Heukseok-ro, Dongjak-gu, Seoul 156-756, Republic of Korea

Supporting Information

ABSTRACT: Both single crystals and pure polycrystalline samples of three new quaternary alkali metal molybdenum selenites, $Na_2Mo_2O_5(SeO_3)_2$, $K_2Mo_2O_5(SeO_3)_2$, and $Rb_2Mo_3O_7(SeO_3)_3$, have been synthesized through hydrothermal and solid-state reactions using A_2CO_3 (A = Na, K, and Rb), MoO_3, and SeO_2 as reagents. The frameworks of all three materials consist of both families of second-order Jahn−Teller distortive cations, i.e., the d^0 cation (Mo^{6+}) and the lone pair cation (Se^{4+}). Although the extent of framework distortions and the resulting occupation sites of alkali metal cations are dissimilar, $Na_2Mo_2O_5(SeO_3)_2$ and $K_2Mo_2O_5(SeO_3)_2$ exhibit similar three-dimensional networks that are composed of highly asymmetric Mo_2O_{11} dimers and SeO_3 polyhedra. $Rb_2Mo_3O_7(SeO_3)_3$ reveals a two-dimensional structure that is built with Mo_3O_{15} trimers and SeO_3 intralayer linkers. Close structural examinations suggest that the structure-directing effect of alkali metal cations is significant in determining the framework distortions and the dimensions of the molybdenum selenites. UV−vis diffuse reflectance and infrared spectroscopy, thermogravimetric analyses, and ion-exchange reactions are reported, as are out-of-center distortion and dipole moment calculations.

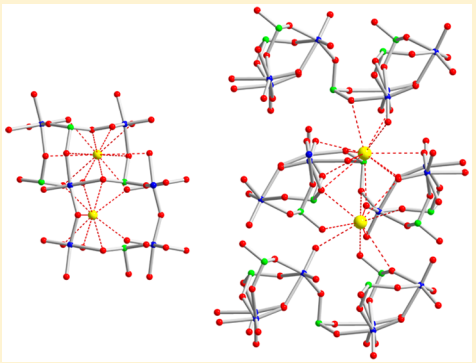

INTRODUCTION

Cations susceptible to electronic second-order Jahn−Teller (SOJT) distortion have been of great interest for chemists discovering novel functional oxide materials.[1] The SOJT distortion takes place if the energy difference between the lowest unoccupied (LUMO) and highest occupied molecular orbital (HOMO) is small and if a mixing of the LUMO and HOMO states can be achieved by a symmetry-allowed distortion. In oxide materials, the two observed families of metal cations revealing a highly unsymmetrical environment owing to the SOJT effect are lone pair cations (Tl^+, Sn^{2+}, Sb^{3+}, Te^{4+}) and octahedrally coordinated d^0 metal cations (Ti^{4+}, V^{5+}, Nb^{5+}, W^{6+}). Combining both families of the SOJT distortive cations has significantly increased the formation of interesting macroscopic noncentrosymmetric (NCS) oxide materials.[2] In addition, many NCS materials have also been found from compounds composed of d^{10} cations and borates.[3] In fact, the NCS oxides are the key host materials in many important applications such as memories, sensors, energy harvesting, optical communications, and detectors attributable to the symmetry-dependent characteristics such as ferroelectricity, pyroelectricity, piezoelectricity, and second-harmonic generation (SHG) behavior.[4] The rational design of the best performing NCS materials is, however, only possible by thorough and careful understanding of local asymmetric polyhedra and their intimate relationships. Several known features strongly influencing the materials' framework structures as well as the macroscopic centricities thus far are the framework flexibility, the hydrogen-bonding, and the cation size effect.[5] In order to obtain further comprehensive insight into the factors determining the variable framework geometries in extended oxide materials with asymmetric building blocks, we have investigated the A^+−Mo^{6+}−Se^{4+}−oxide (A = Na, K, and Rb) system that contains both families of SOJT distortive cations. Several interesting molybdenum selenites have been synthesized and characterized so far.[6] A few oxides such as $A_2(MoO_3)_3SeO_3$ (A = NH_4 and Cs),[6a,h] $BaMo_2O_5(SeO_3)_2$,[6b] Na_2MoSeO_6,[6c] and $Zn_2(MoO_4)(SeO_3)$[6i] are NCS. Herein, we present phase-pure synthesis, structure determination, and characterization of three new molybdenum selenites, $Na_2Mo_2O_5(SeO_3)_2$, $K_2Mo_2O_5(SeO_3)_2$, and $Rb_2Mo_3O_7(SeO_3)_3$. We will demonstrate that the structure-directing effect of alkali metal cations is critical in determining the framework distortions and the dimensions of the molybdenum selenites. Dipole moment and out-of-center distortion calculations for the constituent asymmetric polyhedra and a robust ion-exchange reaction will also be presented.

EXPERIMENTAL SECTION

Reagents. Na_2CO_3 (Hayashi, 99.5%), K_2CO_3 (Jin Chemical, 99.5%), Rb_2CO_3 (Alfa Aesar, 99.8%), MoO_3 (Alfa Aesar, 99.5%), and SeO_2 (Alfa Aesar, 99.4%) were used as received.

Synthesis. Single crystals of all the reported alkali metal molybdenum selenites have been grown hydrothermally. For $A_2Mo_2O_5(SeO_3)_2$ (A = Na and K), 2.00×10^{-3} mol of A_2CO_3, 1.00×10^{-3} mol (0.144 g) of

Received: July 15, 2015
Published: August 26, 2015

DOI: 10.1021/acs.inorgchem.5b01588
Inorg. Chem. 2015, 54, 8832−8839

MoO_3, 4.00×10^{-3} mol (0.444 g) of SeO_2, and 1 mL of water were combined. For $Rb_2Mo_3O_7(SeO_3)_3$, 1.00×10^{-3} mol (0.231 g) of Rb_2CO_3, 1.00×10^{-3} mol (0.144 g) of MoO_3, 4.00×10^{-3} mol (0.444 g) of SeO_2, and 0.5 mL of water were mixed. The reaction mixtures were introduced into separate 23 mL autoclaves with Teflon liners. The autoclaves were tightly sealed, heated to 180 °C [200 °C for $Rb_2Mo_3O_7(SeO_3)_3$] for 4 days, and cooled to room temperature at a rate of 6 °C h^{-1}. After cooling, each reactor was opened and the products were isolated by filtration. Light yellow crystals of $Na_2Mo_2O_5(SeO_3)_2$ and colorless crystals of $K_2Mo_2O_5(SeO_3)_2$ and $Rb_2Mo_3O_7(SeO_3)_3$ were obtained in 95%, 61%, and 57% yields, respectively, based on MoO_3. It should be noted that several efforts to synthesize Cs-containing new molybdenum selenites under similar reaction conditions always resulted in $Cs_2(MoO_3)_3SeO_3$.[6a,h] Pure polycrystalline samples of all the reported materials were also synthesized by standard solid-state reactions. Stoichiometric amounts of the same starting mixtures were ground thoroughly and pressed into pellets. The pellets were transferred into fused silica tubes, which were evacuated and sealed. The tubes were heated to 300 °C for 36 h with two intermediate regrindings. Powder X-ray diffraction (PXRD) data on the resultant polycrystalline products were in very good agreements with the calculated XRD patterns from the single-crystal data (see the Supporting Information).

Single-Crystal X-ray Diffraction. For single-crystal structure determination, a light yellow plate ($0.008 \times 0.089 \times 0.148$ mm^3) for $Na_2Mo_2O_5(SeO_3)_2$, a colorless rod ($0.026 \times 0.032 \times 0.226$ mm^3) for $K_2Mo_2O_5(SeO_3)_2$, and a colorless block ($0.044 \times 0.060 \times 0.062$ mm^3) for $Rb_2Mo_3O_7(SeO_3)_3$ were used. A Bruker SMART BREEZE diffractometer with a 1K CCD area detector and monochromated Mo Kα radiation was used for the data collection. A narrow-frame method was utilized to acquire the data with an exposure time of 10 s/frame and scan widths of 0.30° in ω. The collected data were integrated by the program SAINT.[7] The intensities for obtained data were corrected for polarization, Lorentz factor, air absorption, and absorption due to the deviation through the detector faceplate in the path length. A semiempirical absorption correction was applied on the hemisphere of data using the program SADABS.[8] The data were solved using SHELXS-97[9] and refined with SHELXL-97.[10] For all crystallographic calculations, the WinGX-98 software package was used.[11] Crystallographic data and selected bond distances for $Na_2Mo_2O_5(SeO_3)_2$, $K_2Mo_2O_5(SeO_3)_2$, and $Rb_2Mo_3O_7(SeO_3)_3$ are summarized in Tables 1 and 2.

Table 1. Crystallographic Data for $Na_2Mo_2O_5(SeO_3)_2$, $K_2Mo_2O_5(SeO_3)_2$, and $Rb_2Mo_3O_7(SeO_3)_3$

formula	$Na_2Mo_2Se_2O_{11}$	$K_2Mo_2Se_2O_{11}$	$Rb_2Mo_3Se_3O_{16}$
fw	571.78	604.00	951.64
space group	*I*2/*a* (No. 15)	*Pnma* (No. 62)	$P2_1/c$ (No. 14)
a (Å)	9.37710(10)	10.1954(7)	13.4726(2)
b (Å)	6.44990(10)	14.7619(9)	8.11530(10)
c (Å)	15.2427(2)	6.6972(4)	13.6171(2)
β (deg)	99.252(10)	90	92.112(10)
V ($Å^3$)	909.91(2)	1007.95(11)	1487.80(4)
Z	4	4	4
T (K)	298.0(2)	298.0(2)	298.0(2)
λ (Å)	0.71073	0.71073	0.71073
ρ_{calcd} (g cm^{-3})	4.174	3.980	4.248
$R(F)^a$	0.0304	0.0279	0.0206
$R_w(F_o^2)^b$	0.0818	0.0692	0.0405

$^aR(F) = \sum||F_o| - |F_c||/\sum|F_o|$. $^bR_w(F_o^2) = [\sum w(F_o^2 - F_c^2)^2/\sum w(F_o^2)^2]^{1/2}$.

Powder X-ray Diffraction. PXRD was used to confirm the phase purities of the synthesized materials. The data were obtained on a Bruker D8-Advance diffractometer using Cu Kα radiation at RT with 40 kV and 40 mA. The samples were initially ground well and placed tightly on sample holders. The diffraction data were collected in the 2θ range of 10–70° with a step size of 0.02° and a step time of 0.2 s.

Table 2. Selected Bond Distances (Å) for $Na_2Mo_2O_5(SeO_3)_2$, $K_2Mo_2O_5(SeO_3)_2$, and $Rb_2Mo_3O_7(SeO_3)_3$

$Na_2Mo_2O_5(SeO_3)_2$		$K_2Mo_2O_5(SeO_3)_2$	
Mo(1)–O(1)	1.704(4)	Mo(1)–O(1)	1.7028(19)
Mo(1)–O(2)	1.714(2)	Mo(1)–O(2)	1.715(2)
Mo(1)–O(3)	1.9116(13)	Mo(1)–O(3)	1.9072(8)
Mo(1)–O(4)	2.030(3)	Mo(1)–O(4)	2.0121(17)
Mo(1)–O(5)	2.142(3)	Mo(1)–O(5)	2.185(2)
Mo(1)–O(6)	2.277(2)	Mo(1)–O(6)	2.2580(19)
Se(1)–O(4)	1.733(3)	Se(1)–O(4)	1.7153(17)
Se(1)–O(5)	1.694(2)	Se(1)–O(5)	1.689(2)
Se(1)–O(6)	1.690(2)	Se(1)–O(6)	1.6900(19)
Na(1)–O(2) × 2	2.959(2)	K(1)–O(1) × 2	2.810(2)
Na(1)–O(4) × 2	2.396(3)	K(1)–O(2) × 2	2.7509(18)
Na(1)–O(5) × 2	2.861(2)	K(1)–O(4) × 2	3.235(2)
Na(1)–O(6) × 2	2.500(3)	K(1)–O(4) × 2	3.397(2)
Na(2)–O(1) × 2	2.386(4)	K(1)–O(5) × 2	3.0236(19)
Na(2)–O(2) × 2	2.464(3)	K(1)–O(6) × 2	2.7313(18)
Na(2)–O(3)	2.404(4)	K(2)–O(1) × 2	2.655(2)
Na(2)–O(5) × 2	2.412(3)	K(2)–O(2) × 2	2.999(2)
		K(2)–O(3)	2.826(3)
		K(2)–O(5) × 2	2.7118(19)
		K(2)–O(6) × 2	3.0475(19)
$Rb_2Mo_3O_7(SeO_3)_3$			
Mo(1)–O(1)	1.698(2)	Sc(3)–O(9)	1.717(2)
Mo(1)–O(2)	1.703(2)	Sc(3)–O(14)	1.721(2)
Mo(1)–O(3)	1.947(2)	Rb(1)–O(1)	3.145(2)
Mo(1)–O(4)	1.993(2)	Rb(1)–O(1)	3.204(2)
Mo(1)–O(5)	2.165(2)	Rb(1)–O(2)	3.175(2)
Mo(1)–O(6)	2.307(2)	Rb(1)–O(3)	2.989(2)
Mo(2)–O(6)	1.757(2)	Rb(1)–O(4)	3.400(2)
Mo(2)–O(7)	1.679(2)	Rb(1)–O(5)	3.170(2)
Mo(2)–O(8)	1.898(2)	Rb(1)–O(13)	3.329(3)
Mo(2)–O(9)	2.005(2)	Rb(1)–O(14)	3.021(2)
Mo(2)–O(10)	2.129(2)	Rb(1)–O(16)	2.909(2)
Mo(2)–O(11)	2.318(2)	Rb(1)–O(16)	2.924(2)
Mo(3)–O(8)	1.939(2)	Rb(2)–O(2)	3.152(2)
Mo(3)–O(11)	2.206(2)	Rb(2)–O(6)	3.133(2)
Mo(3)–O(12)	1.689(2)	Rb(2)–O(7)	3.257(2)
Mo(3)–O(13)	1.708(3)	Rb(2)–O(8)	2.893(2)
Mo(3)–O(14)	2.054(2)	Rb(2)–O(8)	3.437(2)
Mo(3)–O(15)	2.229(2)	Rb(2)–O(9)	3.018(2)
Se(1)–O(3)	1.744(2)	Rb(2)–O(10)	3.045(2)
Se(1)–O(10)	1.692(2)	Rb(2)–O(10)	3.369(2)
Se(1)–O(15)	1.670(2)	Rb(2)–O(12)	3.103(3)
Se(2)–O(4)	1.758(2)	Rb(2)–O(13)	3.018(2)
Se(2)–O(11)	1.727(2)	Rb(2)–O(14)	3.525(2)
Se(2)–O(16)	1.617(3)	Rb(2)–O(15)	2.916(2)
Se(3)–O(5)	1.669(2)		

Infrared Spectroscopy. IR spectra were obtained on a Thermo Scientific iS10 FT-IR spectrometer in the spectral range 400–4000 cm^{-1}, with the ground samples intimately contacted by a diamond attenuated total reflectance (ATR) crystal.

UV–Vis Diffuse Reflectance Spectroscopy. UV–vis diffuse reflectance spectra were recorded on a Varian Cary 500 scan UV–vis–NIR spectrophotometer over the spectral range 200–2500 nm at room temperature. The Kubelka–Munk function was used to convert the reflectance spectra to the absorbance data.[12]

Thermogravimetric Analyses. TGA were performed using a Scinco TGA-N 1000 thermal analyzer. The polycrystalline samples were loaded within alumina crucibles and heated to 1000 °C at a rate of 10 °C min^{-1} under flowing argon.

DOI: 10.1021/acs.inorgchem.5b01588
Inorg. Chem. 2015, 54, 8832–8839

Ion-Exchange Experiment. Ion-exchange reaction was carried out by stirring ca. 0.10 g of polycrystalline $K_2Mo_2O_5(SeO_3)_2$ in 0.5 mL of a 4 M aqueous solution of $NaNO_3$. The reaction was performed at 150 °C for 24 h, and the ion-exchanged product was isolated by filtration, washed with plenty of water, and dried in air for 24 h.

Scanning Electron Microscopy/Energy Dispersive Analysis by X-ray (SEM/EDX). A Hitachi S-3400N and a Horiba Energy EX-250 were utilized to perform SEM/EDX. EDX for $Na_2Mo_2O_5(SeO_3)_2$, $K_2Mo_2O_5(SeO_3)_2$, and $Rb_2Mo_3O_7(SeO_3)_3$ reveal approximate A:Mo:Se ratios of 1.0:1.0:1.2, 1.0:0.9:1.0, and 2.0:3.0:3.3, respectively.

RESULTS AND DISCUSSION

Structures. *$Na_2Mo_2O_5(SeO_3)_2$.* $Na_2Mo_2O_5(SeO_3)_2$ is a new quaternary molybdenum selenite that crystallizes in the monoclinic space group *I*2/*a* (No. 15). The framework of $Na_2Mo_2O_5(SeO_3)_2$ consists of highly distorted MoO_6 octahedra and SeO_3 polyhedra (see Figure 1). As seen in Figure 1, the Mo^{6+} cation reveals a cationic displacement from the center of the MoO_6 octahedron in the local C_2 direction, which results in two short [1.704(4)−1.714(2) Å], two intermediate [1.9116(13)−2.030(3) Å], and two long [2.142(3)−2.277(2) Å] Mo−O bonds. The unique Se^{4+} cation is in a trigonal pyramidal coordination environment, connected to three oxygen atoms. The Se−O bond lengths range from 1.690(2) to 1.733(3) Å with O−Se−O bond angles of 95.66(12)−105.20(12)°. Two unique Na^+ cations, $Na(1)^+$ and $Na(2)^+$, are in 8- and 7-fold coordination environments, respectively, within an asymmetric unit with the Na−O contact lengths of 2.386(4)−2.959(2) Å. Two MoO_6 octahedra share their corners through O(3) and form Mo_2O_{11} dimers (see Figure 2a). The corner-shared octahedral dimers are further connected by SeO_3 groups through O(4), O(5), and O(6), which results in a three-dimensional framework (see Figure 2b). Four- (4-MR) and six-membered-ring (6-MR) channels that are running along the [010] direction are observed in the *ac*-plane (see Figure 2b), whereas eight-membered ring (8-MR) channels that are parallel to the [001] direction are monitored in the *ab*-plane (see Figure 2c). The approximate channel dimensions for 4-MR, 6-MR, and 8-MR are 3.0 Å × 4.7 Å [010], 4.9 Å × 6.2 Å [010], and 5.7 Å × 5.7 Å [001], respectively. As seen in Figure 2b and c, while $Na(1)^+$ cations reside in 4-MR channels, $Na(2)^+$ cations exist in 8-MR channels. In connectivity terms, $Na_2Mo_2O_5(SeO_3)_2$ can be represented as an anionic framework of $\{[MoO_{4/2}O_{2/1}]^{2-}\ [SeO_{3/2}]^+\}^-$ with the charge balance maintained by the Na^+ cations. Bond valence sum calculations[13] for Na^+, Mo^{6+}, Se^{4+}, and O^{2-} result in values of 1.00−1.27, 6.07, 3.91, and 1.93−2.23, respectively.

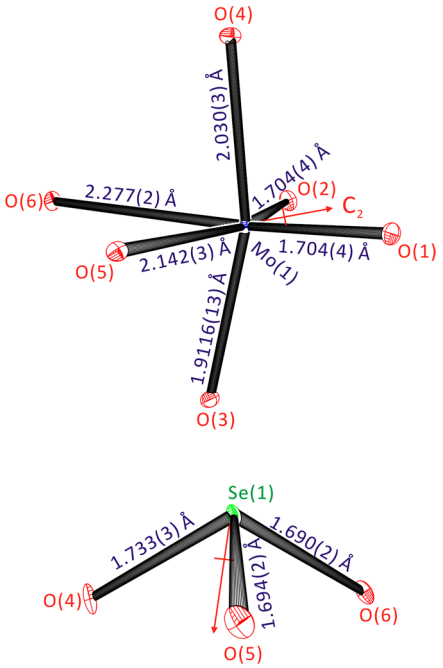

Figure 1. ORTEP (50% probability ellipsoids) representation of a distorted MoO_6 octahedron and an asymmetric SeO_3 trigonal pyramid in $Na_2Mo_2O_5(SeO_3)_2$.

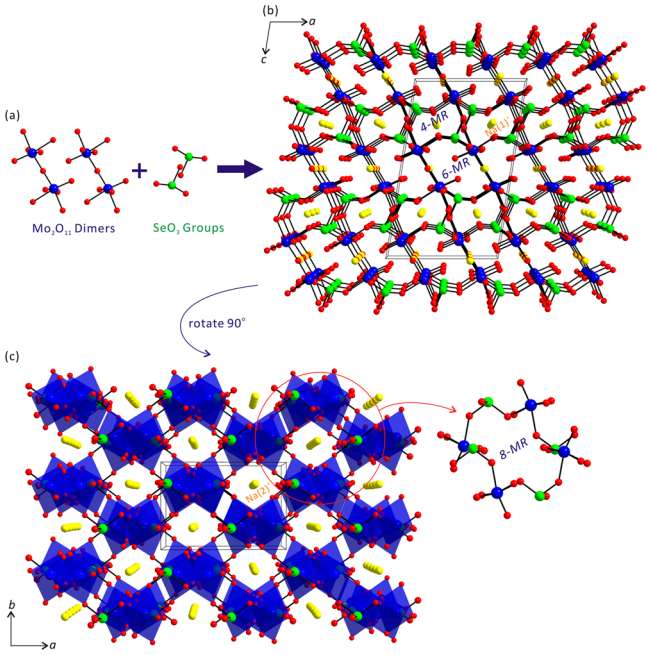

Figure 2. (a) Ball-and-stick model showing the combination of Mo_2O_{11} dimers of corner-shared MoO_6 octahedra and SeO_3 polyhedra in $Na_2Mo_2O_5(SeO_3)_2$ (blue, Mo; green, Se; red, O; yellow, Na). (b) Four- (4-MR) and six-membered-ring (6-MR) channels that are running along the [010] direction are observed in the *ac*-plane. (c) Eight-membered-ring (8-MR) channels that are parallel to the [001] direction are monitored in the *ab*-plane.

$K_2Mo_2O_5(SeO_3)_2$. Another new alkali metal molybdenum selenite, $K_2Mo_2O_5(SeO_3)_2$, crystallizes in the orthorhombic space group *Pnma* (No. 62). $K_2Mo_2O_5(SeO_3)_2$ also exhibits a three-dimensional framework structure that consists of distorted MoO_6 octahedra and asymmetric SeO_3 polyhedra (see Figure 3). Similar to that of $Na_2Mo_2O_5(SeO_3)_2$, the unique Mo^{6+} cation reveals a local C_2 distortion in an octahedral coordination environment with two short [1.7028(19)−1.715(2) Å], two medium [1.9072(8)−2.0121(17) Å], and two long [2.185(2)−2.2580(19) Å] Mo−O bonds. The observed O−Mo−O bond angles are 89.63(14)−179.3(2)°. Within an asymmetric unit, a unique Se^{4+} cation that is connected to three oxygen atoms exists in trigonal pyramidal geometry, i.e., SeO_3. The observed Se−O bond distances and the O−Se−O bond angles are 1.689(2)−1.7153(17) Å and 101.90(9)−104.59(10)°, respectively (see Figure 3). $K(1)^+$ and $K(2)^+$ interact with nine and 12 oxygen atoms, respectively, with K−O contact distances ranging from 2.655(2) to 3.397(2) Å. Two distorted MoO_6 octahedra share their vertices through O(3) and create similar Mo_2O_{11} dimers found in $Na_2Mo_2O_5(SeO_3)_2$ (see Figure 4a). The Mo_2O_{11} dimers are then combined by SeO_3 groups, and another three-dimensional backbone of a molybdenum selenite is produced (see Figure 4b and c). As seen in Figure 4c, the lone pairs on

DOI: 10.1021/acs.inorgchem.5b01588
Inorg. Chem. 2015, 54, 8832−8839

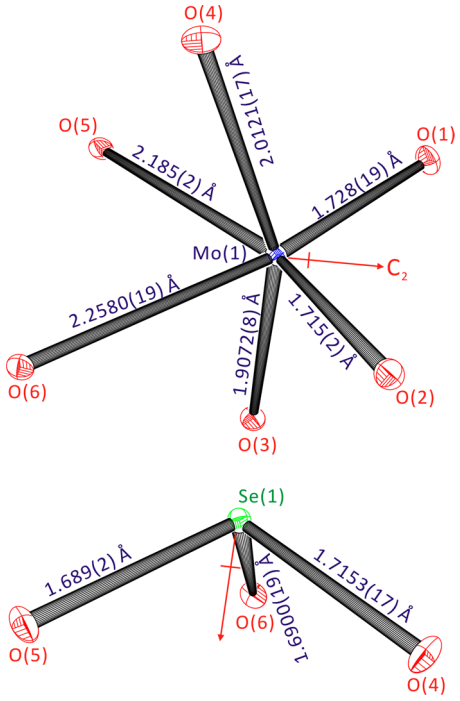

Figure 3. ORTEP (50% probability ellipsoids) drawing of a highly distorted MoO_6 octahedron and an asymmetric SeO_3 group in $K_2Mo_2O_5(SeO_3)_2$.

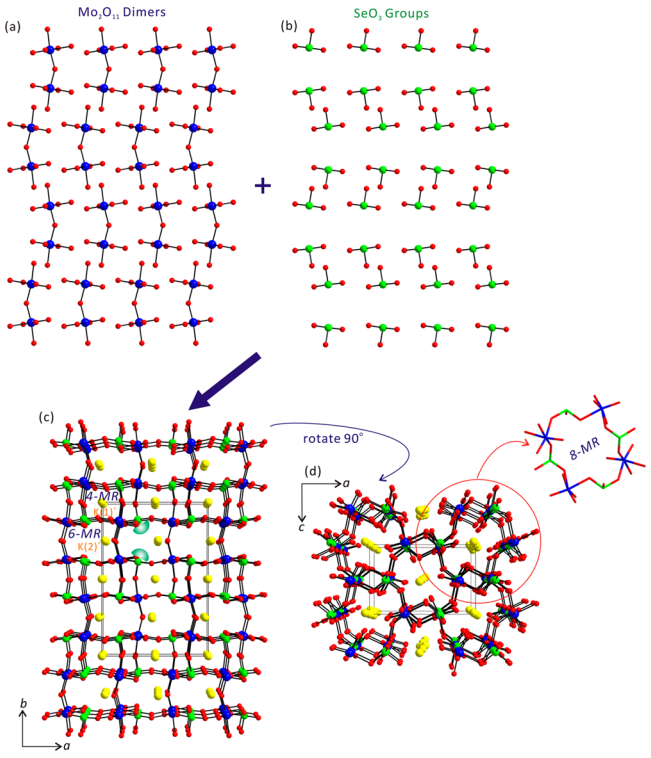

Figure 4. Ball-and-stick representations of (a) Mo_2O_{11} dimers of corner-shared distorted MoO_6 octahedra and (b) asymmetric SeO_3 polyhedra in $K_2Mo_2O_5(SeO_3)_2$ (blue, Mo; green, Se; red, O; yellow, K). (c) 4-MR and 6-MR channels parallel to the [001] direction are observed in the *ab*-plane. (d) 8-MR channels running down to the [010] direction are found in the *ac*-plane.

asymmetric SeO_3 groups are approximately pointing toward the [011] and [0−1−1] directions. While both of the 4-MR and 6-MR channels parallel to the [001] direction are observed in the *ab*-plane, 8-MR channels running down to the [010] direction are found in the *ac*-plane (see Figure 4c). $K(1)^+$ cations exist in 4-MR channels, whereas $K(2)^+$ cations sit in 6-MR channels in the *ab*-plane. Interestingly, all $K(2)^+$ cations flock together in one end within 6-MR channels attributed to the occupation of another end by lone pairs on Se^{4+} cations (see Figure 4c). The dimensions for 4-MR, 6-MR, and 8-MR channels in $K_2Mo_2O_5(SeO_3)_2$ are approximately 3.8 Å × 4.0 Å [001], 4.3 Å × 6.7 Å [001], and 5.5 Å × 6.0 Å [010], respectively. In connectivity terms, the framework of $K_2Mo_2O_5(SeO_3)_2$ may be written as $\{[MoO_{4/2}O_{2/1}]^{2-}[SeO_{3/2}]^+\}^-$ with the charge neutrality retained by the K^+ cations. Bond valences[13] for K^+, Mo^{6+}, Se^{4+}, and O^{2-} are calculated to be 1.24−1.29, 6.07, 3.95, and 1.98−2.20, respectively.

$Rb_2Mo_3O_7(SeO_3)_3$. Although the stoichiometry is different from those of the previous two materials, $Rb_2Mo_3O_7(SeO_3)_3$ is another new quaternary molybdenum selenite that is crystallizing in the monoclinic space group $P2_1/c$ (No. 14). $Rb_2Mo_3O_7(SeO_3)_3$ reveals a lamellar structure that is composed of three unique MoO_6 octahedra and three unique SeO_3 polyhedra (see Figure 5). Interestingly, all three unique MoO_6

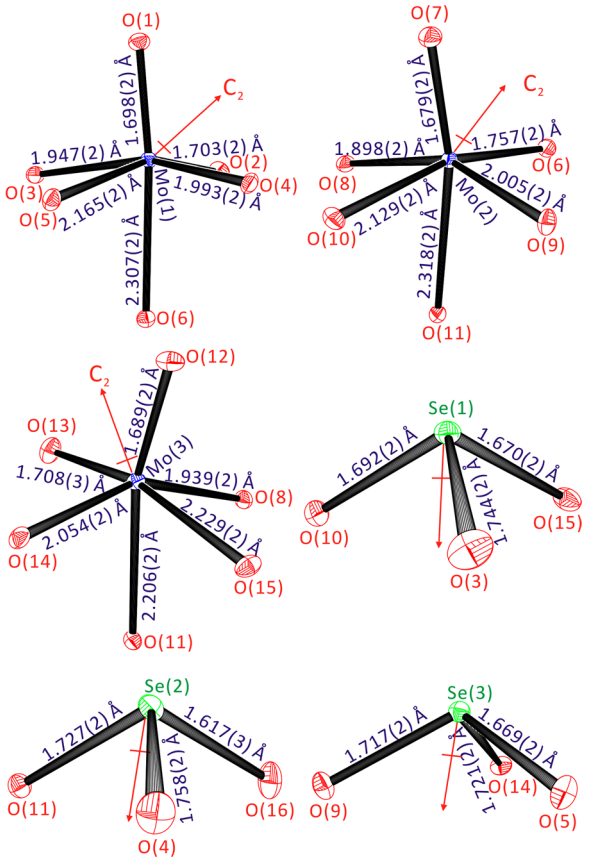

Figure 5. ORTEP (50% probability ellipsoids) drawings of three unique MoO_6 octahedra and three unique SeO_3 trigonal pyramids in $Rb_2Mo_3O_7(SeO_3)_3$.

octahedra show the edge-type C_2 displacement, which is the most frequently observed local octahedral distortion for a Mo^{6+} cation.[14] The Mo−O bond distances in the distorted MoO_6 octahedra range from 1.679(2) to 2.318(2) Å. All three unique Se^{4+} cations are connected to three oxygen atoms in trigonal pyramidal moieties with the Se−O bond distances ranging from 1.617(3) to 1.758(2) Å. Two large alkali metal cations,

DOI: 10.1021/acs.inorgchem.5b01588
Inorg. Chem. 2015, 54, 8832−8839

$Rb(1)^+$ and $Rb(2)^+$, interact with 10 and 12 oxygen atoms, respectively, with the Rb−O contact distances of 2.893(2)−3.525(2) Å. While $Mo(1)O_6$ and $Mo(2)O_6$ octahedra share their corners through O(6), $Mo(2)O_6$ and $Mo(3)O_6$ octahedra share their edges through O(8) and O(11) (see Figure 6a).

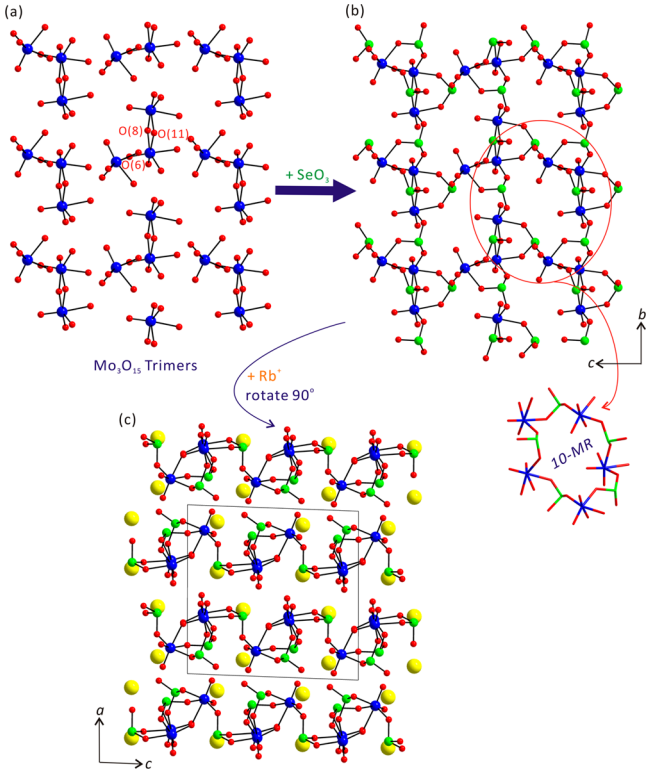

Figure 6. Ball-and-stick models representing (a) the Mo_3O_{15} trimers obtained from the corner- and edge-sharing of three MoO_6 octahedra, (b) linking of SeO_3 groups to form a layered structure in the *bc*-plane, and (c) a complete layered structure of $Rb_2Mo_3O_7(SeO_3)_3$ in the *ac*-plane (blue, Mo; green, Se; red, O; yellow, Rb).

The corner-sharing and edge-sharing of three MoO_6 octahedra result in Mo_3O_{15} trimers. Then the corners of the Mo_3O_{15} trimers are linked by the SeO_3 groups. The linking of SeO_3 groups to the corners of Mo_3O_{15} trimers forms a layered structure in the *bc*-plane. As seen in Figure 6b, here the $Se(1)O_3$ and $Se(3)O_3$ groups are intertrimer linkers, whereas the $Se(2)O_3$ group is an intratrimer connector. Within the layer, small three-membered rings (3-MRs) and large 10-membered rings (10-MRs) are observed (see Figure 6b). Two unique Rb^+ cations reside in between the layers and interact with oxide ligands in the layers (see Figure 6c). The backbone of $Rb_2Mo_3O_7(SeO_3)_3$ can be written as an anionic layer of $\{[Mo(1)O_{4/2}O_{2/1}]^{2-}$ $[Mo(2)O_{4/2}O_{1/3}O_{1/1}]^{0.667-}$ $[Mo(3)O_{3/2}O_{2/1}O_{1/3}]^{1.667-}$ $[Se(1)O_{3/2}]^+$ $[Se(2)O_{1/1}O_{1/2}O_{1/3}]^{0.333+}$ $[Se(3)O_{3/2}]^+\}^{2-}$ with the charge neutrality retained by the Rb^+ cation. Bond valence sum calculations[13] for the Rb^+, Mo^{6+}, Se^{4+}, and O^{2-} reveal values of 0.92−1.05, 6.02−6.09, 3.88−4.01, and 1.85−2.20, respectively.

Infrared Spectroscopy. In order to confirm the particular bonding networks in the reported materials, IR spectra for all three materials have been obtained. The IR spectra for $Na_2Mo_2O_5(SeO_3)_2$, $K_2Mo_2O_5(SeO_3)_2$, and $Rb_2Mo_3O_7(SeO_3)_3$ reveal Mo−O and Se−O vibrations at around 613−669 and 831−974 cm^{-1}, respectively. Peaks occurring at around 464−530 cm^{-1} may be attributable to Mo−O−Mo and Mo−O−Se vibrations. The IR spectral data for all three compounds are found in the Supporting Information. The assignments are in accordance with reported mixed molybdenum and selenium oxide materials.[6,15]

UV−Vis Diffuse Reflectance Spectroscopy. The UV−vis spectral data for the reported solid-state compounds have been measured to calculate their band gaps. The band gaps acquired from the calculations with the Kubelka−Munk function[12] for $Na_2Mo_2O_5(SeO_3)_2$, $K_2Mo_2O_5(SeO_3)_2$, and $Rb_2Mo_3O_7(SeO_3)_3$ result in approximately 3.1, 3.3, and 3.1 eV, respectively. The values have been obtained by extrapolating the straight part of the arising curves to zero in the (K/S) vs E plots, in which K, S, and E are the absorption, the scattering, and the energy, respectively. The observed band gaps should be attributed to both of the distortions arising from SeO_3 groups and the extent of Mo (4d) orbitals participating in the conduction bands in the frameworks. The UV−vis diffuse reflectance spectra for the reported materials are deposited in the Supporting Information.

Thermogravimetric Analysis. The thermal stabilities of the reported materials have been investigated through TGA. All three materials exhibit similar single-step weight losses in the TGA curves attributed to the sublimation of SeO_2 from the frameworks. For $Na_2Mo_2O_5(SeO_3)_2$ and $K_2Mo_2O_5(SeO_3)_2$, two equivalents of SeO_2 are lost at 330 and 370 °C, respectively, calculated (experimental): $Na_2Mo_2O_5(SeO_3)_2$, 38.8% (37.7%); $K_2Mo_2O_5(SeO_3)_2$, 36.7% (37.4%). For $Rb_2Mo_3O_7(SeO_3)_3$, three equivalents of SeO_2 are lost at about 290 °C, calculated (experimental): 35.0% (34.3%). The TGA diagrams for the reported samples are found in the Supporting Information.

Magnitudes of Out-of-Center Distortions and Dipole Moment Calculations. All three reported materials contain a d^0 transition metal cation, Mo^{6+}, in their frameworks. As previously described, all of the Mo^{6+} cations in the reported materials distort toward an edge of their octahedra (local C_2 distortions). In fact, the local C_2 distortion is the most commonly observed intraoctahedral distortion type for a Mo^{6+} cation.[14] The magnitudes of out-of-center distortions (Δ_d) for the MoO_6 octahedra can be quantified by taking into account the six Mo−O bond distances and deviations from 180° of the three *trans* O−Mo−O bond angles. Using the method, the Δ_d values for MoO_6 octahedra in $Na_2Mo_2O_5(SeO_3)_2$, $K_2Mo_2O_5(SeO_3)_2$, and $Rb_2Mo_3O_7(SeO_3)_3$ are calculated to be 1.16, 1.17, and 1.16−1.20, respectively (see Table 3). The values are quite similar to the average magnitude of the intraoctahedral distortion

Table 3. Calculation of Dipole Moments and Magnitudes of Distortions (Δ_d) for Polyhedra in $Na_2Mo_2O_5(SeO_3)_2$, $K_2Mo_2O_5(SeO_3)_2$, and $Rb_2Mo_3O_7(SeO_3)_3$

compound	species	dipole moment (D)[a]	magnitude of distortion (Δ_d)
$Na_2Mo_2O_5(SeO_3)_2$	$Se(1)O_3$	6.8	
	$Mo(1)O_6$	4.5	1.16
$K_2Mo_2O_5(SeO_3)_2$	$Se(1)O_3$	6.0	
	$Mo(1)O_6$	4.6	1.17
$Rb_2Mo_3O_7(SeO_3)_3$	$Se(1)O_3$	7.2	
	$Se(2)O_3$	7.6	
	$Se(3)O_3$	7.8	
	$Mo(1)O_6$	5.9	1.16
	$Mo(2)O_6$	4.9	1.16
	$Mo(3)O_6$	5.7	1.20

[a]D = debyes.

DOI: 10.1021/acs.inorgchem.5b01588
Inorg. Chem. 2015, 54, 8832−8839

(1.21) for Mo^{6+}, which is classified as one of the strongest distorters.[14]

Since the three new molybdenum selenites possess both families of SOJT distortive cations, the extent of distortions for the polyhedra and the subsequent asymmetric coordination environments could be better understood by determining the local dipole moments.[16] The calculated dipole moments for the highly asymmetric MoO_6 and SeO_3 groups are about 4.5−5.9 and 6.0−7.8 D (D = debyes), respectively, which are very similar to those of previously reported molybdenum selenium oxides.[6j,k] The magnitudes of out-of-center distortions and local dipole moments for the asymmetric polyhedra in the reported materials are summarized in Table 3.

Structure-Directing Effect of Alkali Metal Cations. All three reported quaternary alkali metal molybdenum selenites, $Na_2Mo_2O_5(SeO_3)_2$, $K_2Mo_2O_5(SeO_3)_2$, and $Rb_2Mo_3O_7(SeO_3)_3$, crystallize in different space groups. Although $Na_2Mo_2O_5(SeO_3)_2$ and $K_2Mo_2O_5(SeO_3)_2$ are stoichiometrically equivalent, they exhibit distinct framework geometries. A closer structural examination suggests that *the structure-directing effect of alkali metal cations is significant in determining the framework structures* of the molybdenum selenites. Specifically, the smaller cation $Na(1)^+$ (eight-coordinate Na^+, 1.18 Å)[17] in $Na_2Mo_2O_5(SeO_3)_2$ interacts with eight oxygen atoms in the 4-MR (3.0 Å × 4.7 Å) in the *ac*-plane and makes the 4-MR significantly distorted (see Figure 7a).

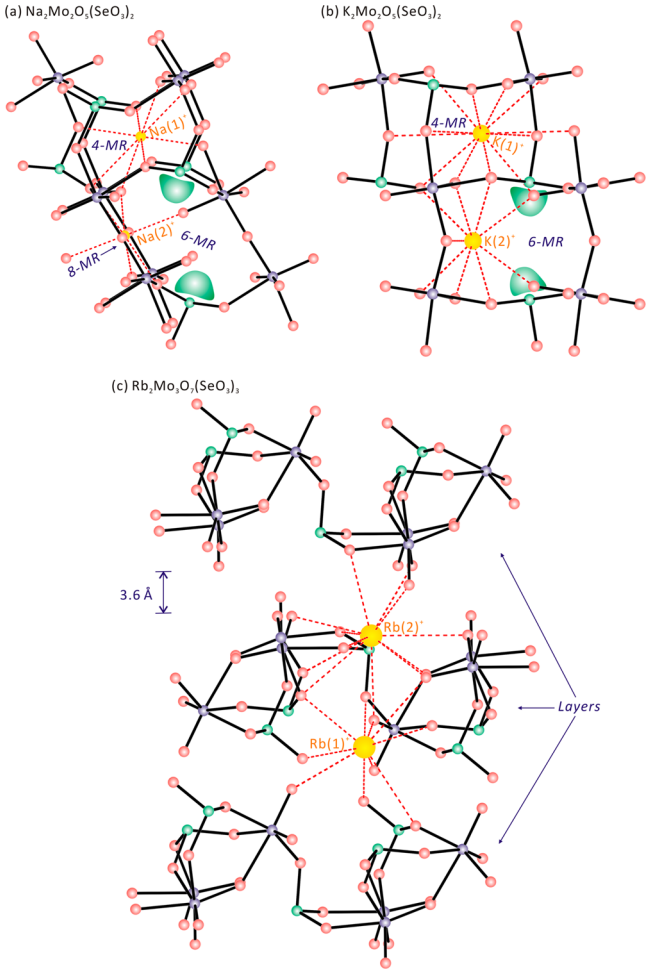

Figure 7. Ball-and-stick models showing the structure-directing effect of alkali metal cations in (a) $Na_2Mo_2O_5(SeO_3)_2$, (b) $K_2Mo_2O_5(SeO_3)_2$, and (c) $Rb_2Mo_3O_7(SeO_3)_3$.

Since the channel dimensions for 6-MRs are too large (4.9 Å × 6.2 Å) for another smaller cation, $Na(2)^+$, in the *ac*-plane, it is difficult for $Na(2)^+$ to interact with oxide ligands in the 6-MR. In addition, lone pairs on the SeO_3 groups that are directing inward impede the residing of $Na(2)^+$ within the 6-MR. Rather the $Na(2)^+$ cation is located in the smaller (5.7 Å × 5.7 Å) helical 8-MR channel in the *ab*-plane and contacts with seven oxygen atoms. $K_2Mo_2O_5(SeO_3)_2$, with a bit larger cations, $K(1)^+$ and $K(2)^+$, reveals a slightly different structural backbone. Similar to that of $Na_2Mo_2O_5(SeO_3)_2$, $K(1)^+$ contacts with nine oxide ligands in the 4-MR in the *ab*-plane. However, the 4-MR is not as twisted out compared to that of the Na analogue, since the coordination environment of K^+ is large enough to interact with nine oxygen atoms in the channel (see Figure 7b; nine-coordinate K^+, 1.55 Å).[17] It is also possible for $K(2)^+$ to reside in the larger 6-MR channel along the [001] direction. The alkali metal cation $K(2)^+$ is large enough to maintain the 6-MR by interacting with 12 oxygen atoms (12-coordinate K^+, 1.64 Å).[17] As seen in Figure 7b, lone pairs on the SeO_3 groups are pointing inward and occupying one end of the 6-MR; thus, all $K(2)^+$ cations are located in another end of the 6-MR. Although $Rb_2Mo_3O_7(SeO_3)_3$ has a different stoichiometry, a similar structure-directing effect of the alkali metal cation is observed. The two unique Rb^+ cations, $Rb(1)^+$ and $Rb(2)^+$, in $Rb_2Mo_3O_7(SeO_3)_3$ have 10- and 12-coordination environments with oxygen atoms, respectively (10-coordinate Rb^+, 1.66 Å; 12-coordinate Rb^+, 1.72 Å).[17] Since the larger Rb^+ cations can interact with many oxide ligands, Mo_3O_{15} trimers and more SeO_3 groups may be found around the coordination environment. Attributable to the huge size of Rb^+ cations, the closest interlayer O−O contact is 3.6 Å (Figure 7c). Thus, the large coordination environment of Rb^+ pushes the layers apart and the SeO_3 groups in $Rb_2Mo_3O_7(SeO_3)_3$ serve as intralayer linkers. Similar structure-directing effects of the cations influencing the dimensions of the frameworks have been observed from other mixed metal selenites and tellurites such as $A_2(MoO_3)_3(SeO_3)$ (A = Rb, Tl, Cs, and NH_4)[6a,h] and $A_2TeW_3O_{12}$ (A = K, Rb, and Cs).[18]

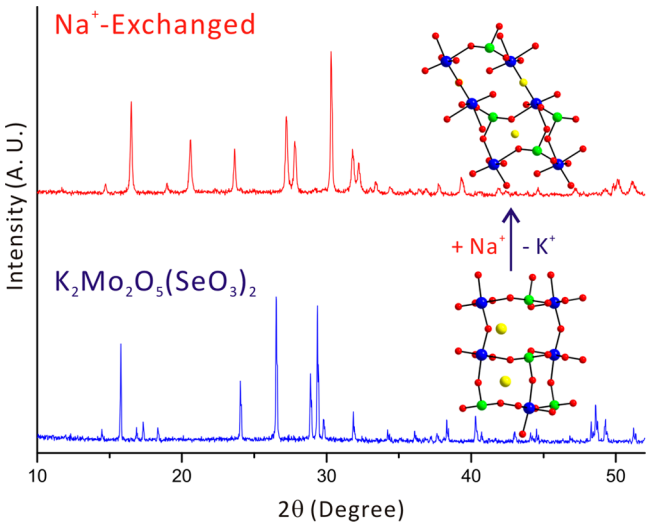

Figure 8. Powder X-ray diffraction patterns (Cu Kα radiation) of $K_2Mo_2O_5(SeO_3)_2$ (bottom) and the product of the ion exchange of $K_2Mo_2O_5(SeO_3)_2$ with the Na^+ (top) cation. Note the framework of the orthorhombic $K_2Mo_2O_5(SeO_3)_2$ changes to the monoclinic $Na_2Mo_2O_5(SeO_3)_2$ through the ion exchange.

DOI: 10.1021/acs.inorgchem.5b01588
Inorg. Chem. 2015, 54, 8832−8839

Ion-Exchange Experiment. Since $K_2Mo_2O_5(SeO_3)_2$ contains 4-, 6-, and 8-MR channels in the framework, the K^+ cation within the channels may be replaced by the smaller cation Na^+ through ion-exchange reactions. The ion-exchange reaction performed by stirring polycrystalline $K_2Mo_2O_5(SeO_3)_2$ in a 4 M aqueous solution of $NaNO_3$ for 1 day at 150 °C exhibited a robust ion-exchange behavior. Interestingly, the powder X-ray diffraction pattern for the ion-exchanged product is very similar to that of $Na_2Mo_2O_5(SeO_3)_2$. EDX analysis on the exchanged product reveals that more than 90% of K^+ cations have been replaced by Na^+ cations. As seen in Figure 8, the framework of $K_2Mo_2O_5(SeO_3)_2$ with the orthorhombic crystal class has been completely transformed to that of monoclinic $Na_2Mo_2O_5(SeO_3)_2$ through the ion-exchange reaction.

CONCLUSIONS

Three new quaternary alkali metal molybdenum selenium oxides, $Na_2Mo_2O_5(SeO_3)_2$, $K_2Mo_2O_5(SeO_3)_2$, and $Rb_2Mo_3O_7(SeO_3)_3$, have been synthesized by hydrothermal and solid-state reactions. Stoichiometrically equivalent $Na_2Mo_2O_5(SeO_3)_2$ and $K_2Mo_2O_5(SeO_3)_2$ represent three-dimensional frameworks that are composed of highly distorted Mo_2O_{11} dimers and SeO_3 polyhedra. Whereas the $Na(2)^+$ cation in $Na_2Mo_2O_5(SeO_3)_2$ resides in the smaller helical 8-MR channel, the $K(2)^+$ cation in $K_2Mo_2O_5(SeO_3)_2$ is situated in the larger 6-MR channel. $Rb_2Mo_3O_7(SeO_3)_3$ reveals a layered structure consisting of Mo_3O_{15} trimers and SeO_3 intralayer linkers. Detailed structural analyses suggest that the templating effect of variable alkali metal cations is critical in determining the framework geometry and the dimensions of the new molybdenum selenites. Many open channels in $K_2Mo_2O_5(SeO_3)_2$ permit the facile ion exchange of Na^+ along with the framework transformation.

ASSOCIATED CONTENT

Supporting Information

The Supporting Information is available free of charge on the ACS Publications website at DOI: 10.1021/acs.inorgchem.5b01588.

Calculated and observed X-ray diffraction patterns, thermogravimetric analysis diagrams, infrared spectra, and UV−vis diffuse reflectance spectra for $Na_2Mo_2O_5(SeO_3)_2$, $K_2Mo_2O_5(SeO_3)_2$, and $Rb_2Mo_3O_7(SeO_3)_3$ (PDF)

X-ray crystallographic file in CIF format (CIF)

AUTHOR INFORMATION

Corresponding Author

*Phone: +82-2-820-5197. Fax: +82-2-825-4736. E-mail: kmok@cau.ac.kr.

Notes

The authors declare no competing financial interest.

ACKNOWLEDGMENTS

This work was supported by the National Research Foundation of Korea (NRF) grant funded by the Korea government (MSIP) (No. 2013R1A2A2A01007170).

REFERENCES

(1) (a) Opik, U.; Pryce, M. H. L. *Proc. R. Soc. London, Ser. A* **1957**, *A238*, 425−447. (b) Bader, R. F. W. *Can. J. Chem.* **1962**, *40*, 1164−1175. (c) Pearson, R. G. *J. Am. Chem. Soc.* **1969**, *91*, 4947−4955. (d) Pearson, R. G. *J. Mol. Struct.: THEOCHEM* **1983**, *103*, 25−34. (e) Wheeler, R. A.; Whangbo, M.-H.; Hughbanks, T.; Hoffmann, R.; Burdett, J. K.; Albright, T. A. *J. Am. Chem. Soc.* **1986**, *108*, 2222−2236.

(2) (a) Ra, H.-S.; Ok, K. M.; Halasyamani, P. S. *J. Am. Chem. Soc.* **2003**, *125*, 7764−7765. (b) Chen, X. A.; Zhang, L.; Chang, X. N.; Xue, H. P.; Zang, H. G.; Xiao, W. Q.; Song, X. M.; Yan, H. *J. Alloys Compd.* **2007**, *428*, 54−58. (c) Chang, H. Y.; Kim, S.-H.; Halasyamani, P. S.; Ok, K. M. *J. Am. Chem. Soc.* **2009**, *131*, 2426−2427. (d) Chang, H. Y.; Kim, S.-H.; Ok, K. M.; Halasyamani, P. S. *Chem. Mater.* **2009**, *21*, 1654−1662. (e) Sun, C. F.; Hu, C. L.; Xu, X.; Ling, J. B.; Hu, T.; Kong, F.; Long, X. F.; Mao, J.-G. *J. Am. Chem. Soc.* **2009**, *131*, 9486−9487. (f) Yang, B. P.; Hu, C. L.; Xu, X.; Sun, C. F.; Zhang, J. H.; Mao, J.-G. *Chem. Mater.* **2010**, *22*, 1545−1550. (g) Lee, D. W.; Oh, S.-J.; Halasyamani, P. S.; Ok, K. M. *Inorg. Chem.* **2011**, *50*, 4473−4480. (h) Sun, C. F.; Hu, C. L.; Xu, X.; Yang, B. P.; Mao, J.-G. *J. Am. Chem. Soc.* **2011**, *133*, 5561−5572. (i) Nguyen, S. D.; Halasyamani, P. S. *Inorg. Chem.* **2012**, *51*, 9529−9538. (j) Nguyen, S. D.; Halasyamani, P. S. *Inorg. Chem.* **2013**, *52*, 2637−2647. (k) Kim, Y. H.; Lee, D. W.; Ok, K. M. *Inorg. Chem.* **2014**, *53*, 5240. (l) Cao, X. L.; Hu, C. L.; Kong, F.; Mao, J.-G. *Inorg. Chem.* **2015**, *54*, 3875−3882.

(3) (a) Pan, S.; Smit, J. P.; Watkins, B.; Marvel, M. R.; Stern, C. L.; Poeppelmeier, K. R. *J. Am. Chem. Soc.* **2006**, *128*, 11631−11634. (b) Wu, H.; Pan, S.; Poeppelmeier, K. R.; Li, H.; Jia, D.; Chen, Z.; Fan, X.; Yang, Y.; Rondinelli, J. M.; Luo, H. *J. Am. Chem. Soc.* **2011**, *133*, 7786−7790. (c) Shi, Y.; Pan, S.; Dong, X.; Wang, Y.; Zhang, M.; Zhang, F.; Zhou, Z. *Inorg. Chem.* **2012**, *51*, 10870−10875. (d) Yang, B.-P.; Hu, C.-L.; Xu, X.; Huang, C.; Mao, J.-G. *Inorg. Chem.* **2013**, *52*, 5378−5384. (e) Zhao, S. G.; Luo, J. H.; Zhou, P.; Zhang, S. Q.; Sun, Z. H.; Hong, M. C. *RSC Adv.* **2013**, *3*, 14000−14006. (f) Xu, X.; Hu, C.-L.; Kong, F.; Zhang, J.-H.; Mao, J.-G.; Sun, J. *Inorg. Chem.* **2013**, *52*, 5831−5837. (g) Fan, X.; Zang, L.; Zhang, M.; Qiu, H.; Wang, Z.; Yin, J.; Jia, H.; Pan, S.; Wang, C. *Chem. Mater.* **2014**, *26*, 3169−3174. (h) Song, J.-L.; Hu, C.-L.; Xu, X.; Kong, F.; Mao, J.-G. *Angew. Chem., Int. Ed.* **2015**, *54*, 3679−3682.

(4) (a) Nye, J. F. *Physical Properties of Crystals*; Oxford Univ. Press: Oxford, U.K., 1957. (b) Jona, F.; Shirane, G. *Ferroelectric Crystals*; Pergamon Press: Oxford, 1962. (c) Cady, W. G. *Piezoelectricity; an Introduction to the Theory and Applications of Electromechanical Phenomena in Crystals*; Dover: New York, 1964. (d) Lang, S. B. *Sourcebook of Pyroelectricity*; Gordon & Breach Science: London, 1974. (e) Ok, K. M.; Chi, E. O.; Halasyamani, P. S. *Chem. Soc. Rev.* **2006**, *35*, 710−717.

(5) (a) Sykora, R. E.; Ok, K. M.; Halasyamani, P. S.; Albrecht-Schmitt, T. E. *J. Am. Chem. Soc.* **2002**, *124*, 1951−1957. (b) Chang, H. Y.; Kim, S. H.; Ok, K. M.; Halasyamani, P. S. *J. Am. Chem. Soc.* **2009**, *131*, 6865−6873. (c) Choi, M.-H.; Kim, S.-H.; Chang, H. Y.; Halasyamani, P. S.; Ok, K. M. *Inorg. Chem.* **2009**, *48*, 8376−8382. (d) Lee, D. W.; Bak, D.-b.; Kim, S. B.; Kim, J.; Ok, K. M. *Inorg. Chem.* **2012**, *51*, 7844−7850. (e) Oh, S.-J.; Lee, D. W.; Ok, K. M. *Inorg. Chem.* **2012**, *51*, 5393−5399. (f) Lee, D. W.; Ok, K. M. *Inorg. Chem.* **2013**, *52*, 5176−5184. (g) Kim, Y. H.; Lee, D. W.; Ok, K. M. *Inorg. Chem.* **2014**, *53*, 1250−1256. (h) Kim, Y. H.; Thao, T. T.; Halasyamani, P. S.; Ok, K. M. *Inorg. Chem. Front.* **2015**, *2*, 361−368.

(6) (a) Harrison, W. T. A.; Dussack, L. L.; Jacobson, A. J. *Inorg. Chem.* **1994**, *33*, 6043−6049. (b) Harrison, W. T. A.; Dussack, L. L.; Jacobson, A. J. *J. Solid State Chem.* **1996**, *125*, 234−242. (c) Porter, Y.; Halasyamani, P. S. *J. Solid State Chem.* **2003**, *174*, 441−449. (d) Shen, Y. L.; Jiang, H. L.; Xu, J.; Mao, J.-G.; Cheah, K. W. *Inorg. Chem.* **2005**, *44*, 9314−9321. (e) Jiang, H.; Xie, Z.; Mao, J.-G. *Inorg. Chem.* **2007**, *46*, 6495−6501. (f) Ling, J.; Albrecht Schmitt, T. E. *J. Solid State Chem.* **2007**, *180*, 1601−1607. (g) Zhang, S.; Jiang, H.; Sun, C.; Mao, J.-G. *Inorg. Chem.* **2009**, *48*, 11809−11820. (h) Chang, H. Y.; Kim, S. W.; Halasyamani, P. S. *Chem. Mater.* **2010**, *22*, 3241−3250. (i) Nguyen, S. D.; Kim, S. H.; Halasyamani, P. S. *Inorg. Chem.* **2011**, *50*, 5215−5222. (j) Oh, S.-J.; Lee, D. W.; Ok, K. M. *Dalton Trans.* **2012**, *41*, 2995−3000. (k) Bang, S.-e.; Pan, Z.; Kim, Y. H.; Lee, D. W.; Ok, K. M. *J. Solid State Chem.* **2013**, *208*, 65−70.

(7) *SAINT*, A Program for Area Detector Absorption Correction, version 4.05; Siemens Analytical X-ray Instruments: Madison, WI, 1995.

(8) Blessing, R. H. *Acta Crystallogr., Sect. A: Found. Crystallogr.* **1995**, *51*, 33−38.

DOI: 10.1021/acs.inorgchem.5b01588
Inorg. Chem. 2015, 54, 8832−8839

(9) Sheldrick, G. M. *SHELXS-97* - A program for automatic solution of crystal structures; University of Goettingen: Goettingen, Germany, 1997.
(10) Sheldrick, G. M. *SHELXL-97* - A program for crystal structure refinement; University of Goettingen: Goettingen, Germany, 1997.
(11) Farrugia, L. J. *J. Appl. Crystallogr.* **1999**, *32*, 837−838.
(12) (a) Kubelka, P.; Munk, F. *Z. Technol. Phys.* **1931**, *12*, 593. (b) Tauc, J. *Mater. Res. Bull.* **1970**, *5*, 721−729.
(13) (a) Brown, I. D.; Altermatt, D. *Acta Crystallogr., Sect. B: Struct. Sci.* **1985**, *B41*, 244−247. (b) Brese, N. E.; O'Keeffe, M. *Acta Crystallogr., Sect. B: Struct. Sci.* **1991**, *B47*, 192−197.
(14) Halasyamani, P. S. *Chem. Mater.* **2004**, *16*, 3586−3592.
(15) Balraj, V.; Vidyasagar, K. *Inorg. Chem.* **1999**, *38*, 5809−5813.
(16) (a) Galy, J.; Meunier, G. *J. Solid State Chem.* **1975**, *13*, 142−159. (b) Maggard, P. A.; Nault, T. S.; Stern, C. L.; Poeppelmeier, K. R. *J. Solid State Chem.* **2003**, *175*, 27−33. (c) Izumi, H. K.; Kirsch, J. E.; Stern, C. L.; Poeppelmeier, K. R. *Inorg. Chem.* **2005**, *44*, 884−895.
(17) Shannon, R. D. *Acta Crystallogr., Sect. A: Cryst. Phys., Diffr., Theor. Gen. Crystallogr.* **1976**, *A32*, 751.
(18) Goodey, J.; Ok, K. M.; Broussard, J.; Hofmann, C.; Escobedo, F. V.; Halasyamani, P. S. *J. Solid State Chem.* **2003**, *175*, 3−12.

DOI: 10.1021/acs.inorgchem.5b01588
Inorg. Chem. 2015, 54, 8832−8839